

**This is the accepted manuscript version of the contribution published as:**

**Krause, S., Goss, K.-U.** (2021):

Could chemical exposure and bioconcentration in fish be affected by slow binding kinetics in blood?

*Environ. Sci.-Proc. Imp.* **23** (5), 714 - 722

**The publisher's version is available at:**

<http://dx.doi.org/10.1039/D1EM00056J>

1  
2  
3  
4  
5  
6  
7  
8  
9  
10  
11  
12  
13  
14

**Could chemical exposure and bioconcentration in fish be affected by slow binding kinetics in blood?**

Sophia Krause<sup>a,\*</sup>, Kai-Uwe Goss<sup>a,b</sup>

<sup>a</sup> Helmholtz Centre for Environmental Research, Department of Analytical Environmental Chemistry, Permoserstr. 15, 04318 Leipzig, Germany

<sup>b</sup> University of Halle-Wittenberg, Institute of Chemistry, Kurt-Mothes-Str. 2, 06120 Halle, Germany

\*Address correspondence to [sophia.krause@ufz.de](mailto:sophia.krause@ufz.de)

15 **Abstract**

16 The possible implications of slow binding kinetics on respiratory uptake, bioconcentration and  
17 exposure of chemicals were evaluated in the present study. Most physiological and chemical  
18 information needed for such an evaluation is already known from the literature or can be  
19 estimated. However, data for binding kinetics in fish plasma between unbound and bound  
20 fraction of chemicals have not been reported in the literature yet.

21 In the first part of this study, we therefore experimentally investigated the plasma binding  
22 kinetics for ten chemicals, including pollutants like polycyclic aromatic hydrocarbons and a  
23 pesticide. The determined desorption rate constants were in the range of 0.4 1/s to 0.1 1/s. In  
24 the second part of this study, we present a comparative modeling analysis of generic  
25 predictions with binding kinetics of different velocities. For doing so, a model that explicitly  
26 represents binding kinetics in blood was developed and applied for different hypothetical  
27 scenarios.

28 The evaluation showed that slow sorption kinetics only limits respiratory uptake and thus  
29 influences the levels of bioaccumulation for extreme and, by that, rather unlikely parameter  
30 combinations (i.e. for strongly sorbing chemicals with very slow binding kinetics). It can  
31 therefore be assumed that limitations on respiratory uptake due to slow binding kinetics in  
32 blood are rather unlikely for most chemicals.

33

34 Keywords: Bioaccumulation, plasma binding, toxicokinetic modeling

35

36 **Introduction**

37 The use of predictive models for screening or assessment of chemicals regarding their  
38 bioaccumulation potential is regarded as a promising approach to reduce the use of animal  
39 testing. Particularly the prediction of bioconcentration factors (BCFs) has recently been subject  
40 of various studies<sup>1-5</sup> because the BCF is an accepted regulatory endpoint. One important  
41 aspect for the predictive performance of such models is the consideration of elimination via  
42 biotransformation. For obtaining reliable estimates of biotransformation kinetics, so-called *in*  
43 *vitro* biotransformation assays were developed and refined in recent years, and finally two  
44 OECD test guidelines on this topic have been published<sup>6, 7</sup>. The so determined *in vitro* rate  
45 constants are then mathematically converted into corresponding *in vivo* rate constants that can  
46 be used in BCF prediction models by appropriate scaling. Another important aspect for an  
47 accurate prediction of BCFs is the appropriate representation of chemical uptake. The  
48 importance of accurate uptake estimates has led to the development of plenty of methods for  
49 estimating uptake rate constants. A comprehensive overview of existing methods for  
50 estimation of respiratory uptake rate constants is provided by Brooke et al.<sup>8</sup>. In their study,  
51 Brooke et al. concluded that it is difficult to recommend one specific method for prediction of

52 respiratory uptake because several methods showed similar performance. However, even the  
53 “best” performing methods showed notable uncertainty (standard deviations of about 0.5 log-  
54 units), making the estimation of respiratory uptake a major source of uncertainty in BCF  
55 prediction. In general, the respiratory uptake rate depends on ventilation, permeation of the  
56 chemical into gill blood and the capacity of the gill blood to transport the chemical into the body.  
57 When present in blood, most of the chemicals tend to bind to blood components like proteins  
58 and lipids; especially for hydrophobic chemicals where the freely dissolved chemical fraction  
59 in blood is usually small. Commonly, it is assumed that binding of the chemical to blood  
60 components is an instantaneous process. However, if the assumption of instantaneous binding  
61 was incorrect and sorption kinetics was slow, this could have consequences for the transport  
62 capacity of the blood and the subsequent processes in the organism. Especially in the  
63 pharmaceutical literature, different experimental approaches have been developed for  
64 investigation of binding kinetics<sup>9-12</sup> and the topic has already gained much attention with a  
65 strong focus on potential implications of slow binding kinetics for drug elimination and  
66 distribution within the body<sup>13-18</sup>. In general, these studies demonstrate that, in most cases,  
67 binding kinetics is faster than the subsequent pharmacokinetic processes so that limitations of  
68 drug elimination or distribution due to slow binding kinetics can be regarded as unlikely.  
69 However, analogous to the potential effects on chemical elimination and distribution, slow  
70 binding kinetics could also affect chemical uptake. To our knowledge, this topic has not yet  
71 been systematically evaluated. In this study, we want to focus on potential effects of slow  
72 binding kinetics on respiratory uptake in fish. For the scenario of respiratory uptake in fish, slow  
73 binding kinetics in blood would mean that the blood could not exploit its full capacity to transport  
74 the chemical from the gills into the periphery and thus could not keep up a high chemical  
75 gradient between ventilated water and gill tissue. As a consequence, less chemical could be  
76 taken up into the gills and one would expect lower chemical concentrations in the organism  
77 compared to a scenario with instantaneous binding in blood. By this, slow binding kinetics  
78 could lead to lower levels of bioaccumulation in the organism. The question whether and to  
79 what extent these effects occur for realistic parameter combinations is what we want to discuss  
80 in this study.

81 For this purpose, we combine experimental data on binding kinetics in fish plasma with suitable  
82 modeling approaches to evaluate the implications of slow binding kinetics on respiratory  
83 uptake of chemicals in fish. To investigate how fast binding kinetics in plasma is, the desorption  
84 kinetics of a set of organic chemicals (including polycyclic aromatic hydrocarbons and  
85 substituted benzenes) was determined experimentally using a recently described method<sup>19</sup>.  
86 This method for experimental determination of desorption rate constants involves the time-  
87 resolved extraction of the test chemicals from rainbow trout plasma. The use of plasma instead  
88 of whole blood in the experiments is due to the better handling Regarding partitioning, plasma

89 is generally considered a suitable surrogate for whole blood<sup>20</sup>. However, we cannot completely  
90 exclude the possibility that kinetics of specific sorption processes to individual components of  
91 whole blood may differ from those to plasma components. Combination of the determined  
92 desorption rate constants with the corresponding equilibrium constants for plasma binding of  
93 the chemicals allows for derivation of the rate constants for the reverse process (i.e. for  
94 sorption to the plasma components). The derived kinetic information is then used to assess  
95 whether binding kinetics in plasma limits respiratory uptake of chemicals. For the quantitative  
96 evaluation of the impact of binding kinetics on respiratory uptake of chemicals, a model  
97 structure that incorporates binding kinetics in blood was developed and compared with a  
98 simpler model that assumes instantaneous binding equilibrium. We apply the model for  
99 different parameter combinations to gain a general mechanistic understanding of the influence  
100 of binding kinetics on chemical uptake and bioaccumulation.

101 For clarity, we want to start with some –often misinterpreted- theories and concepts that are  
102 frequently brought up in discussions on the exchange kinetics between blood and neighboring  
103 compartments. For example, the idea often arises that the bound fraction of a chemical could  
104 also be available for uptake into eliminating tissues or for uptake by degrading enzymes in  
105 contrast to the otherwise accepted paradigm that only the freely dissolved fraction of a  
106 chemical is relevant. Some authors thus insinuate that, the actual available amount of  
107 chemical may actually be greater than conceptually represented in the models that refer to the  
108 unbound fraction<sup>21-23</sup>. In fact, however, theoretical considerations show that models which  
109 refer to freely dissolved chemical concentrations already reflect the availability of the bound  
110 fraction. If instantaneous sorption in blood is assumed, this conceptually means that free  
111 molecules removed from the blood are immediately replaced by molecules from the bound  
112 state. It does not matter whether one assumes that freely dissolved chemical is taken up or  
113 whether a direct uptake of bound chemical (i.e. without the chemical transitioning into the freely  
114 dissolved state) is also possible. By assuming instantaneous equilibrium between free and  
115 bound chemical, the underlying information is redundant. Thus, it is conceptually irrelevant  
116 whether one refers to the freely dissolved fraction when quantifying elimination (which is the  
117 typical approach) or whether one refers to the bound fraction. Thought through consistently,  
118 both approaches (no matter which reference is used) lead to the same result in the end. The  
119 only exception are models that assume the bound fraction to be irreversibly bound and, by this,  
120 not available for uptake under any circumstances.

121 Another reasoning suggests that protein facilitated transport of the bound chemical could  
122 enhance chemical uptake<sup>21, 23, 24</sup>, e.g. the uptake from blood into biotransforming tissues like  
123 the liver. Facilitated transport is therefore sometimes suggested as an explanation for why *in*  
124 *vitro*-based predictions underestimate *in vivo* biotransformation. Various studies have shown  
125 that the phenomenon of facilitated transport can indeed increase uptake or exchange rate of a

126 chemical between two phases<sup>25-27</sup>. A prerequisite for this effect, however, is that the exchange  
127 of the freely dissolved chemical has been kinetically limited in the first place<sup>27, 28</sup>. Exactly this  
128 point does not apply to the classical models of chemical elimination, such as those used e.g.  
129 for *in vitro* – *in vivo* extrapolation of hepatic biotransformation data. These models<sup>3, 29</sup> make  
130 the simplifying assumption that the exchange of the chemical between blood and eliminating  
131 tissue is instantaneous. Facilitated transport as an explanation why these models  
132 underestimate hepatic elimination is thus not applicable, because no process can become  
133 faster than instantaneous.

134 Thus, on the subject of sorption in blood, arguments are sometimes put forward for observed  
135 discrepancies between model-based BCF predictions and *in vivo* measurements that are not  
136 consistent with the actual concepts/models applied<sup>20, 30</sup>. The model applied here takes into  
137 account a kinetic limitation between bound and unbound chemical in blood, but does not  
138 represent any further kinetic limitation for the permeation of the chemical into surrounding  
139 tissues, such as slow membrane permeability. Consequently, free molecules removed from  
140 the blood are replaced by molecules from the bound state according to the prevailing kinetics  
141 but acceleration of chemical uptake from blood into tissues due to facilitated transport does  
142 not apply here, because this exchange process is *a priori* assumed to be instantaneous.

143

## 144 **Methods**

145

### 146 Experiments for determination of desorption kinetics

147 For determination of desorption kinetics, time-resolved extractions of the test chemicals (see  
148 Table 1) from diluted rainbow trout plasma were performed as described elsewhere<sup>19</sup>. In short,  
149 200 µL of the plasma solution spiked with test chemical were pumped through the capillary  
150 with defined flow rates (24 – 0.2 mL/h) using a syringe pump (VIT-FIT syringe pump, Lambda  
151 Laboratory Instruments). Rainbow trout plasma was provided from the Toxicology Centre of  
152 the University of Saskatchewan and a protein content of 21.5 mg/mL was given for undiluted  
153 plasma. Depending on the estimated partition behavior of the test chemicals (see SI section 1  
154 for details on the estimation of the required partition coefficients), different dilution factors for  
155 the plasma were chosen to ensure a) a high bound fraction of the chemical in the plasma  
156 solution and b) a sufficient capacity of the PDMS for nearly complete extraction of the chemical  
157 from the plasma solution in the capillary. For each test chemical, the experiment was  
158 performed twice using differently diluted plasma solutions (used plasma dilutions for each  
159 chemical see SI section 1). The purpose of this procedure is to confirm the determined rate  
160 constants because the kinetics should be independent from the used plasma concentration.  
161 For dilution of the plasma, Cortland's saline (124 mM NaCl, 5.1 mM KCl, 3.0 mM  
162 NaH<sub>2</sub>PO<sub>4</sub>·H<sub>2</sub>O, 11.9 mM NaHCO<sub>3</sub>, 0.94 mM MgSO<sub>4</sub>·7H<sub>2</sub>O, 1.6 mM CaCl<sub>2</sub>·2H<sub>2</sub>O, 10 mM

163 HEPES, pH 7.8) was used. Stock solutions of the chemicals were prepared in methanol or in  
164 isopropanol and spiked into the diluted plasma (used chemical concentrations see SI section  
165 1). The solvent content in the final plasma solution did not exceed 0.5 v/v %. For equilibration,  
166 the spiked plasma solutions were incubated on a roller mixer over night at 11 °C.  
167 The PDMS coated capillary used in the experiments was purchased from Quadrex Corporation  
168 (007-1, inner diameter 0.25 mm, layer 8 µm of 100 % polydimethylsiloxane). A PDMS coated  
169 fiber (Polymicro Technologies Inc., diameter of the glass core 0.123 mm, layer 30 µm of 100  
170 % polydimethylsiloxane) was inserted into the capillary to further increase the PDMS sorption  
171 capacity and reduce the diffusion path lengths inside the capillary. Pieces of 20 cm length of  
172 capillary and fiber were used for the experiments. After passage through the capillary, the  
173 capillary effluent was collected and extracted under gentle shaking for 3 min with 1 mL  
174 cyclohexane for concentration determination. To compare the determined concentrations with  
175 the initial concentrations, samples of the original spiked plasma solution ( not pumped through  
176 the capillary) was also extracted with cyclohexane in the same manner. Extraction efficiency  
177 for each chemical was calculated based on the chemicals' physico-chemical properties and  
178 was > 99 % for all test chemicals. The concentration determination was performed via GC-MS  
179 (7890A/5975C, Agilent Technologies, injection in cold splitless mode, separation with an HP-  
180 5MS column from Agilent Technologies).

181

#### 182 Data evaluation of the desorption experiments

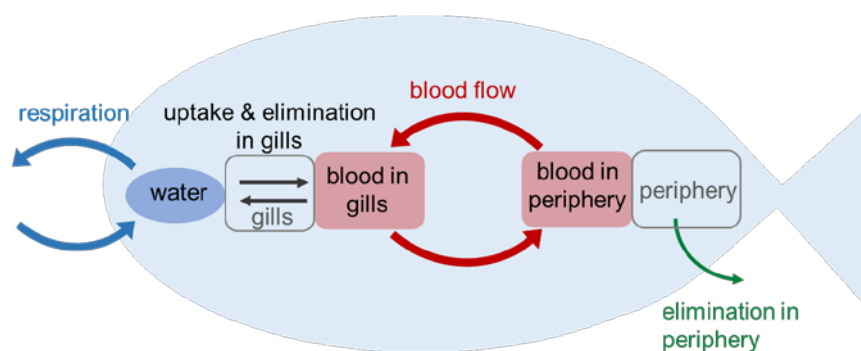
183 The concentrations of the test chemical in the capillary effluent relative to the initial  
184 concentrations were plotted over the corresponding residence times inside the capillary to yield  
185 concentration-time-profiles. The desorption rate constants of the chemicals were determined  
186 from these concentration-time-profile via fitting a transport model that considers convection  
187 and dispersion as well as the partitioning kinetics between sorbing components of plasma and  
188 PDMS. For a detailed description of the transport model we refer to a recently published paper  
189 using the same experimental method and data analysis procedure for determining the  
190 desorption kinetics from albumin <sup>19</sup>. In order to adapt the transport model for the here  
191 performed experiments with plasma, the albumin compartment of the original model <sup>19</sup> was  
192 replaced by a compartment, which represents the total of all sorbing plasma components.  
193 Thus, the heterogeneous individual components of the plasma (e.g. different proteins or  
194 lipoproteins) were combined to a single joint compartment. As mentioned above, the  
195 partitioning constants of the chemicals towards this compartment were estimated using the  
196 approach presented by Endo et al. <sup>31</sup> (see SI section 1) and adjusted based on the generated  
197 concentration-time profiles. Adjustment of the partition coefficients based on the two generated  
198 concentration-time profiles for each chemical (differing in the used plasma dilution) is possible  
199 because the results for the shortest and longest residences inside the capillary are governed

200 by the partition properties <sup>19</sup>. It is not surprising that these adjustments are necessary  
201 considering the fact that the data used to estimate the partition coefficients are not fish derived,  
202 e. g. for partitioning into the trout plasma proteins the partitioning to bovine albumin was used  
203 as surrogate.

204

### 205 Modeling approaches for quantitative evaluation of the impact of binding kinetics

206 To investigate the influence of binding kinetics in gill blood on chemical uptake, two steady-  
207 state models are developed for a fish living under constant exposure to contaminated water  
208 but eating uncontaminated food. One model represents a scenario with binding kinetics in  
209 blood, the other model represents a scenario with instantaneous chemical equilibrium in blood  
210 between the bound state (at transport proteins or lipids) and the freely dissolved state and is  
211 illustrated in Figure 1.



212

213 Figure 1: Schematic overview of the modelled processes. Illustrated is the model that assumes instantaneous  
214 equilibrium in blood. Chemical uptake, elimination and exchange via blood flow are modelled as kinetic processes;  
215 instantaneous equilibrium between gills and gill blood and between periphery and peripheral blood is assumed.

216 The model that considers binding kinetics in blood additionally distinguishes bound and freely  
217 dissolved chemical in the blood compartments; a detailed illustration of this model can be found  
218 in SI section 2b. Both steady-state models represent uptake and elimination of the chemical  
219 via ventilation and transport of the chemical into the periphery of the organism with the blood  
220 flow. Additionally, elimination of the chemical in the periphery, e.g. via fecal egestion or hepatic  
221 biotransformation, is also represented in both models. Both models rely on individual mass  
222 balances for the represented compartments (see SI section 2). Both models are expressed as  
223 linear systems of equations and solved in MS Excel using matrix functions (MMULT, MINV) for  
224 steady state. As a result, the steady-state concentrations of the chemical in the ventilated water  
225 flowing out of the gills, in blood flowing out of the gills and into the gills and in the periphery of  
226 the fish are calculated.

227 For quantification of the impact of sorption kinetics, we use the resulting steady-state  
228 concentrations to calculate uptake efficiency ( $E_{\text{uptake}}$ ), elimination efficiency ( $E_{\text{elimination}}$ ) and  
229 bioconcentration factor (BCF) as a measure of bioaccumulation. The steady-state uptake



230 efficiency  $E_{\text{uptake}}$  describes to which extent a chemical is taken up from the respired water  
 231 and is calculated from the steady-state concentrations of the chemical in the respired water  
 232 flowing into and out of the gills,  $C_{W,\text{in}}$  and  $C_{W,\text{out}}$ :

233

$$E_{\text{uptake}} \equiv \frac{C_{W,\text{in}} - C_{W,\text{out}}}{C_{W,\text{in}}} \quad (1)$$

234

235 The steady-state elimination efficiency  $E_{\text{elimination}}$  in contrast describes to which extent a  
 236 chemical is removed from blood due to elimination in the periphery (e.g. via biotransformation).  
 237 The elimination efficiencies for freely dissolved chemical and bound chemical in blood have to  
 238 be calculated separately using the corresponding steady-state concentrations in blood flowing  
 239 into and out of the periphery ( $C_{\text{blood-free}}$  and  $C_{\text{blood-bound}}$ ).

240

$$E_{\text{elimination}}^{\text{free}} \equiv \frac{C_{\text{blood-free,gills}} - C_{\text{blood-free,periphery}}}{C_{\text{blood-free,gills}}} \quad (2)$$

241

242

$$E_{\text{elimination}}^{\text{bound}} \equiv \frac{C_{\text{blood-bound,gills}} - C_{\text{blood-bound,periphery}}}{C_{\text{blood-bound,gills}}} \quad (3)$$

243

244 These two elimination efficiencies can then be combined to yield the total elimination efficiency  
 245 considering sorption kinetics in blood:

246

$$E_{\text{elimination}}^{\text{total}} = f_{\text{unbound}} * E_{\text{elimination}}^{\text{free}} + f_{\text{bound}} * E_{\text{elimination}}^{\text{bound}} \quad (4)$$

247

248 The BCF is calculated by combining the steady-state concentrations in the different body  
 249 compartments ( $C_{\text{gills}}$ ,  $C_{\text{periphery}}$ ,  $C_{\text{blood,periphery}}$ ,  $C_{\text{blood,gills}}$ ) with the corresponding volume  
 250 information to derive the steady-state whole-body concentration (see SI section 2 for details).

251

$$BCF = \frac{(C_{\text{gills}}V_{\text{gills}} + C_{\text{periphery}}V_{\text{periphery}} + C_{\text{blood,gills}}V_{\text{blood,gills}} + C_{\text{blood,periphery}}V_{\text{blood,periphery}})}{C_{W,\text{in}}} \quad (5)$$

252

### 253 Input data required for model application

254 By default, a 10 g rainbow trout with 5 % body fat at 15 °C was modelled. For application of  
 255 the developed models, physiological data (e.g. blood flow rates, ventilation rate, composition  
 256 of gill tissue, blood and the rest of the organism) are required. The used parameter values are  
 257 described in SI section 3.

258 Furthermore, partition coefficients for chemical partitioning into gills, periphery and within blood  
259 are required. We here use simple approaches based on the octanol-water partition coefficient  
260  $K_{OW}$  for estimation of these partition coefficients because it generates a better general intuitive  
261 understanding about how hydrophobicity affects the outcome of the model results. We note  
262 that a more precise way for estimating tissue partition coefficients is based on the pp-LFER  
263 approach <sup>31</sup> but this approach is only applicable to cases of actual chemicals and, by that, not  
264 suitable for a generic analysis. The partition coefficients for the different tissues are calculated  
265 based on log  $K_{OW}$  analogous to the approach from Saunders et al. <sup>32</sup>:

$$K_{\text{tissue/water}} = \text{lipid}_{\text{tissue}} * K_{OW} + \text{protein}_{\text{tissue}} * 0.05 * K_{OW} + \text{water}_{\text{tissue}} \quad (6)$$

266 In this equation,  $\text{protein}_{\text{tissue}}$  is the protein content of the tissue of interest (as volume fraction  
267 mL/mL),  $\text{lipid}_{\text{tissue}}$  is the lipid content of the tissue of interest (as volume fraction) and  $\text{water}_{\text{tissue}}$   
268 the water content of the tissue of interest (composition data is presented in SI section 3).

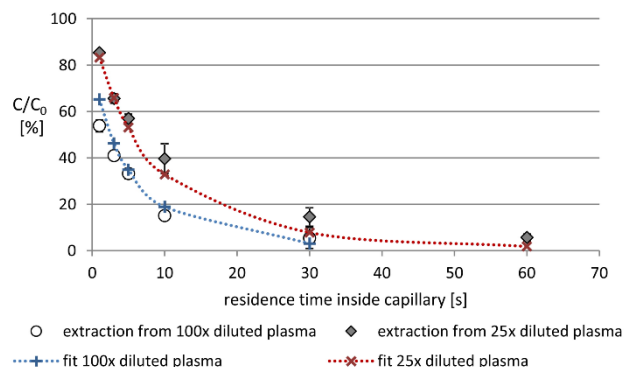
269 The uptake kinetics of chemicals from the respiration water into the blood was estimated via  
270 their respective permeabilities. It was assumed that a barrier consisting of aqueous boundary  
271 layers (ABL), mucus, cell membranes and cytosol must be overcome for uptake into the blood.  
272 Separate permeabilities were calculated for each of the individual layers of this barrier, which  
273 were then used to estimate the total permeability ( $P_{\text{gills}}$ ) in the gills. A detailed description of  
274 the used parameters values and equations for estimating the permeability is also provided in  
275 SI section 3.

276

## 277 **Results & discussion**

### 278 Experimental dataset on sorption kinetics in plasma

279 The desorption experiments yield concentration-time profiles showing the test chemical  
280 concentration after passage through the capillary relative to the initial concentration. These  
281 concentration-time profiles result from the chemical being extracted from the plasma solution  
282 into the PDMS as soon as the chemical desorbs from the binding components in plasma during  
283 passage through the capillary. By this, the concentration-time profiles allow the determination  
284 of desorption rate constants via fitting. As an example the data for extraction of 1,8-  
285 dibromooctane from 25x and 100x fold diluted plasma is shown in Figure 2. Plotted are average  
286 values of duplicates and standard deviations are indicated as error bars. Figure 2 shows that  
287 for both plasma dilutions the concentration of 1,8-dibromooctane was almost zero after 30s or  
288 60 s residence time inside the capillary, respectively. The generated data were modeled with  
289 the developed transport model and a desorption rate constant of 0.2 1/s was determined.



290  
 291 Figure 2: Extraction of 1,8-dibromooctane from plasma. Different plasma dilutions are indicated as diamonds (25x  
 292 dilution) and dots (100x dilution). Shown are mean values of duplicates, standard deviations are indicated as error  
 293 bars. In cases where error bars are invisible, they are covered by the symbols. Corresponding fits with desorption  
 294 rate constants  $k_{des} = 0.2$  1/s are indicated as crosses with interpolated lines between the calculated data points.

295  
 296 The determined desorption rate constants for all tested chemicals are summarized in Table 1.  
 297 The corresponding sorption rate constants can be determined from the equilibrium constant  
 298 and the determined desorption rate constant without the need for further experiments (see SI  
 299 section 4) and are also included in Table 1.

300  
 301 Table 1: Summary of the determined desorption and sorption rate constant ( $k_{des}$  and  $k_{sorb}$ ) and the corresponding  
 302 partition coefficients between sorbing plasma components and water ( $K_{sorbcomp/w}$ ).

test chemical	$\log K_{OW}$ [L/L]	$k_{des}$ [1/s]	$k_{sorb}$ [ $L_W/L_{sorb\ comp}/s$ ]	$\log K_{sorbcomp/w}$ fitted [L/L]
phenanthrene	4.4	0.3	1699	3.75
n-propylbenzene	3.7	0.2	40	2.30
1,8-dibromooctane	4.8	0.2	1133	3.75
1,2,3,4-tetrachlorobenzene	4.6	0.4	1412	3.55
di-n-pentylether	4.3	0.15	75	2.70
n-hexylbenzene	5.3	0.1	600	3.78
chlorpyrifos	5.2	0.1	400	3.60
1,4-dibromobenzene	3.8	0.3	165	2.74
pyrene	4.6	0.15	1800	4.08
1,2,4-trichlorobenzene	4.1	0.2	80	2.60

303  
 304 All determined desorption rate constants are in a range of 0.1 1/s to 0.4 1/s. By that, the here  
 305 determined desorption rate constants are at the lower end of the range of desorption rate  
 306 constants measured with the same method for bovine albumin (0.2 – 1.8 1/s)<sup>19</sup>. The desorption  
 307 rate constants for albumin varied up to one order of magnitude and were directly related to  
 308 molecular weight of the chemicals: The desorption rate constants for rainbow trout plasma  
 309 constituents seem to be located within a narrow range without any clear correlation to

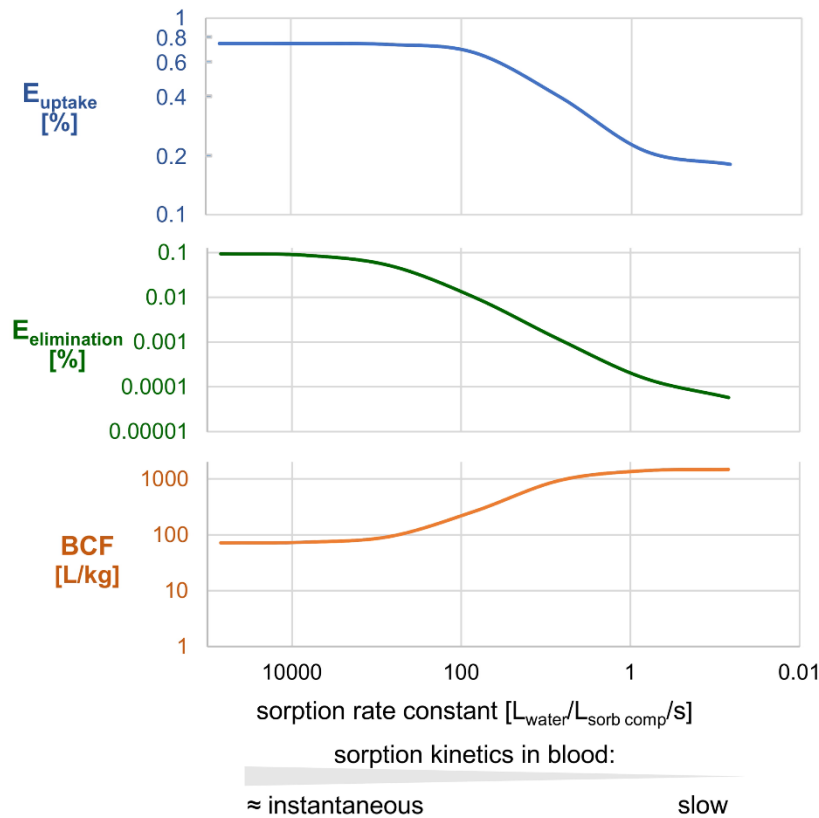
310 molecular properties of the sorbing chemicals. The reason for this could be the following:  
311 Different from the situation with albumin, the sorbing components in plasma are not a  
312 homogeneous sorption phase but a mixture of different proteins and lipoproteins. Accordingly,  
313 the different sorption processes could have different kinetics. In the used data analysis  
314 procedure, however, these different sorption processes are not resolved but a single joint  
315 kinetics is fitted because resolution of all involved sorption processes is not feasible.

316

#### 317 Modeled impacts of sorption kinetics in blood on uptake, elimination and BCF.

318 We calculated the uptake efficiency, elimination efficiency and the BCF with the model  
319 considering sorption kinetics in blood for varying sorption rate constants. The evaluated range  
320 of sorption rate constants was not limited to the experimentally determined values, but a much  
321 greater theoretical range was evaluated to elaborate general effects. Furthermore, we  
322 represent different scenarios in terms of chemical hydrophobicity and elimination via  
323 biotransformation kinetics by varying assumed  $\log K_{OW}$  and biotransformation rate constants  
324 (biotransformation is assumed to occur only in the periphery, not in gills or blood). The purpose  
325 of these simulations is to gain a basic mechanistic understanding of the underlying processes.  
326 These simulations represent various general scenarios and are not substance-specific  
327 calculations, we thus do not provide conclusions on model uncertainty for specific chemicals.  
328 In Figure 3, we exemplarily show the modeled effects of slow sorption kinetics for a scenario  
329 of a chemical with a  $\log K_{OW} = 6$  and a whole-body elimination rate constant  $k_2$  of 4 1/d. This  
330 whole-body elimination rate constant was estimated from an *in vitro* biotransformation rate  
331 constant of 10 1/h using a recently published *in vitro-in vivo* extrapolation tool <sup>1</sup>. Given the  
332 typical range of *in vitro* biotransformation rate constants <sup>33</sup>, a value of 10 1/h already represents  
333 a scenario of fast biotransformation. Thus, limitations are already more likely for this scenario  
334 than for other scenarios with slower elimination, because limitations by slow binding kinetics  
335 become strongest when the other kinetic processes are fast compared to the binding kinetics.

336



337

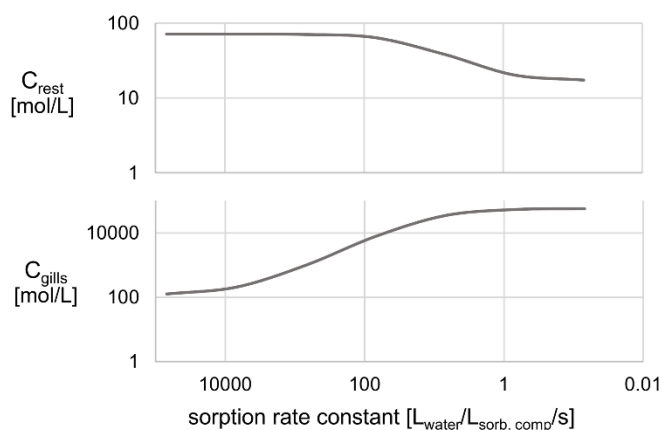
338

339 Figure 3: Change in uptake efficiency ( $E_{\text{uptake}}$ ), elimination efficiency ( $E_{\text{elimination}}$ ) and bioconcentration factor (BCF)  
 340 for a scenario of a chemical with a  $\log K_{\text{OW}} = 6$  and a whole-body elimination rate constant of 4 1/d depending on  
 341 the sorption kinetics in blood.

342 Figure 3 shows that for sorption rate constants higher than 10000  $L_{\text{W}}/L_{\text{sorb comp}}/s$  there are no  
 343 effects on uptake and elimination efficiency and thus neither on the BCF. In a range of sorption  
 344 rate constants between 10000  $L_{\text{W}}/L_{\text{sorb comp}}/s$  and 100  $L_{\text{W}}/L_{\text{sorb comp}}/s$ , a strong decrease in  
 345 elimination efficiency is observed (by one order of magnitude). The reason for this is that slow  
 346 binding kinetics limit the delivery of the chemical into the eliminating tissues in the periphery of  
 347 the organism, because bound chemical must first desorb into the freely dissolved state before  
 348 it can permeate into the eliminating tissues. A decreased elimination can lead to higher BCF  
 349 values because the chemical is less efficiently cleared. Figure 3, however, shows that the BCF  
 350 changes only slightly (from  $\approx 70$  to  $\approx 150$  L/kg) for this range of sorption rate constants. The  
 351 uptake efficiency remains nearly unchanged in the range of sorption rate constants between  
 352 10000  $L_{\text{W}}/L_{\text{sorb comp}}/s$  and 100  $L_{\text{W}}/L_{\text{sorb comp}}/s$ .

353 For sorption rate constants smaller than 100  $L_{\text{W}}/L_{\text{sorb comp}}/s$ , the elimination efficiency declines  
 354 further. In addition, there are now also effects on uptake efficiency and BCF: The uptake  
 355 efficiency shows a decrease from  $\approx 0.8$  to  $\approx 0.2$  for slower sorption rate constants, while the  
 356 BCF increases up to  $\approx 1500$  L/kg for slower sorption kinetics. The uptake efficiency of the  
 357 chemical decreases because the onward transport of the chemical into the rest of the body is

358 limited when sorption of the chemical to the binding components of blood (lipids, proteins) is  
 359 slow. The chemical then accumulates in the gill tissue which leads to a decreasing chemical  
 360 gradient between gill tissue and ventilated water and thus the uptake efficiency reduces. The  
 361 fact that the increase in BCF occurs simultaneously to the decrease in uptake efficiency does  
 362 not seem plausible at first, because one would expect that a lower uptake leads to decreased  
 363 BCF values. The steady-state concentration in the rest of the body  $C_{rest}$  (Figure 4) does indeed  
 364 show that  $C_{rest}$  decreases as soon as the uptake efficiency decreases, so there is less chemical  
 365 in the rest body. The steady-state concentration in the gills ( $C_{gills}$ ), however, shows a strong  
 366 increase as soon as the uptake efficiency decreases indicating that the chemical accumulates  
 367 strongly in the gills (Figure 4). The resulting concentration increase in the gills is so extreme  
 368 that it causes the observed increase of the BCF. Note that if (contrary to what is assumed here)  
 369 significant biotransformation occurred in the gills, such an increase in concentration would not  
 370 be observed in the gills.



371  
 372  
 373 Figure 4: Change in the steady-state concentrations in gills and rest body ( $C_{gills}$  and  $C_{rest}$ ) for a scenario of a  
 374 chemical with a log  $K_{ow}$  = 6 and a whole-body elimination rate constant of 4 1/d depending on sorption kinetics in  
 375 blood.

376 Apart from the potential implications for bioaccumulation, the above results could also be of  
 377 relevance for toxicity assessments, *in vitro-in vivo* extrapolation of toxicity information or  
 378 exposure modelling. Figure 4 shows that for slow sorption kinetics the chemical concentration  
 379 in the gills increases dramatically. A model neglecting sorption kinetics could not predict these  
 380 high chemical concentrations in gill tissue. Accordingly, neglecting sorption kinetics could  
 381 erroneously lead to the indication that the concentration is not high enough to cause toxic  
 382 effects while in fact the concentration could be far above the threshold for toxicity in specific  
 383 organs.

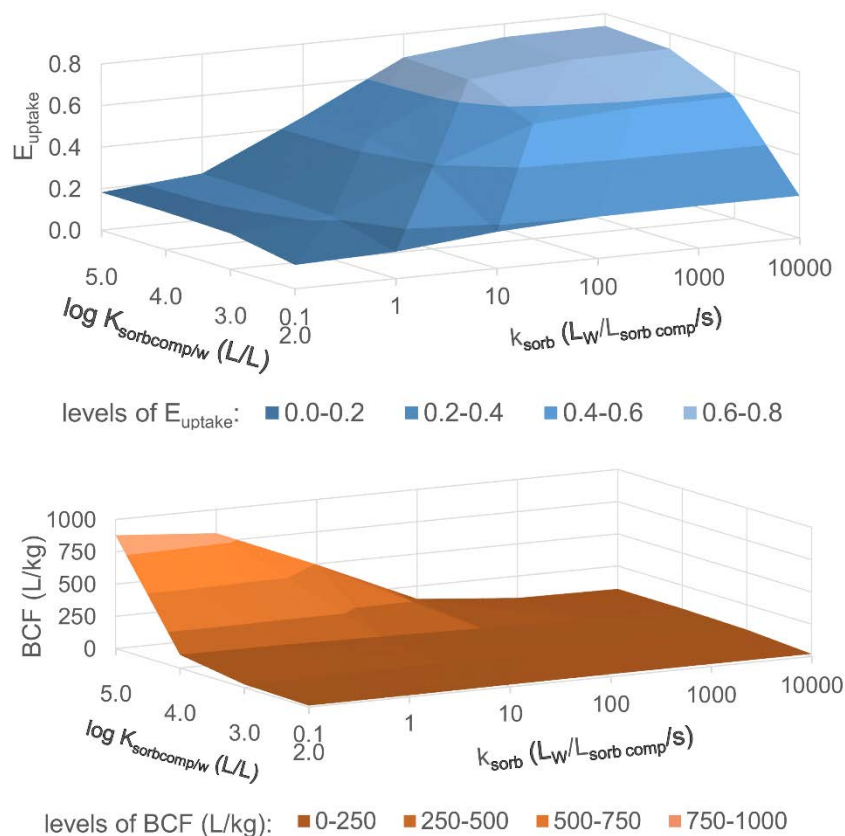
384  
 385 The effects described above also occur in scenarios with other elimination rate constants in a  
 386 similar way, but the numerical values are shifted. For example, in case one arbitrarily assumes

387 a tenfold slower whole-body elimination rate constant of 0.4 1/d (data shown in SI section 5),  
 388 there still is a decrease in elimination and uptake efficiency for slower sorption rate constant  
 389 leading to increasing BCF values. However, while for the above example with a whole-body  
 390 elimination rate constant of 4 1/d  $E_{\text{elimination}}$  decreases up to 3 orders of magnitude and the BCF  
 391 increases by more than one order of magnitude for slow sorption rate constants, the effects  
 392 are smaller for a scenario with a whole-body elimination rate constant of 0.4 1/d:  $E_{\text{elimination}}$   
 393 reduces up to two orders of magnitude and the BCF increases only by factor 2 – 3 (Table 2).  
 394 The reason for these observations is the fact that a potential limitation due to slow binding  
 395 kinetics in blood becomes most relevant when subsequent processes (e.g. elimination) are  
 396 fast compared to the binding kinetics.

397 Table 2: Change of elimination efficiency ( $E_{\text{elimination}}$ ) and bioconcentration factor (BCF) for slow sorption rate  
 398 constants depending on the assumed whole-body elimination rate constants.

resulting effect	whole-body elimination rate constant	
	4 1/d	0.4 1/d
reduction of $E_{\text{elimination}}$	up to 3 orders of magnitude (from 0.1 to 0.0001)	up to 2 orders of magnitude (from 0.01 to 0.0001)
increase of BCF	> one order of magnitude (from 70 L/kg to 1500 L/kg)	by factor 2 - 3 (from 700 L/kg to 1600 L/kg)

399  
 400 For scenarios with log  $K_{\text{OW}}$  values other than 6 analogous effects can be observed, however,  
 401 the impact of sorption kinetics decreases with decreasing log  $K_{\text{OW}}$ . Less hydrophobic  
 402 chemicals have a lower tendency to bind to blood components and thus the impact of sorption  
 403 kinetics also becomes less important. Figure 5 illustrates the relation between sorption rate  
 404 constant, partition coefficient and either uptake efficiency (Figure 5 upper panel) or BCF  
 405 (Figure 5 lower panel), respectively.



406  
 407 Figure 5: Calculation of the uptake efficiency ( $E_{\text{uptake}}$ ) and bioconcentration factor (BCF) in dependency of the  
 408 partition coefficient between sorbing plasma components and water  $K_{\text{sorbcomp/w}} \text{ (L/L)}$  and the sorption rate constant  
 409  $k_{\text{sorb}} \text{ (L}_W\text{/L}_{\text{sorb comp}}\text{/s)}$ .

410 Figure 5 shows that the less hydrophobic a chemical is, the smaller is the impact of sorption  
 411 kinetics on uptake efficiency and BCF: For a chemical with a  $\log K_{\text{sorbing components/water}} = 5 \text{ L}_W\text{/L}_{\text{sorb}}$   
 412  $\text{comp}$ , the uptake efficiency reduces from  $\approx 0.8$  to  $\approx 0.2$  for the here evaluated range of  $k_{\text{sorb}}$ ,  
 413 while the uptake efficiency for a chemical with  $\log K_{\text{sorbing components/water}} = 2 \text{ L}_W\text{/L}_{\text{sorb comp}}$  changes  
 414 only slightly from  $\approx 0.2$  to  $\approx 0.1$  for the same range of  $k_{\text{sorb}}$ . The same can be observed for the  
 415 BCF; the BCF for a chemical with a  $\log K_{\text{sorbing components/water}} = 5$  changes notably for the  
 416 evaluated  $k_{\text{sorb}}$  range while the BCF for a chemical with a  $\log K_{\text{sorbing components/water}} = 2$  remains  
 417 nearly constant. The explanation for this observation is that for less hydrophobic chemicals  
 418 only a small proportion of chemical in the blood actually binds to the sorbing components and  
 419 thus the sorption kinetics cannot have a great influence. The corresponding graph for  
 420 elimination efficiency shows analogous effects and can be found in SI section 6.

421  
 422 Considering both, the determined sorption rate constants and the sorbing plasma components-  
 423 water partition coefficients, one now can evaluate whether a significant limitation of uptake or  
 424 elimination due to sorption kinetics is to be expected for the above test chemicals. The slowest  
 425 sorption rate constants were derived for n-propylbenzene, di-n-pentylether and 1,2,4-  
 426 trichlorobenzene (Table 1). At the same time, however, the sorbing blood components-water



427 partition coefficients for these chemicals are in the low range (log K = 2 – 3, Table 1), so that  
428 for none of the test chemicals a significant limitation of uptake or elimination due to sorption  
429 kinetics is to be expected (Figure 5). Considering all relevant factors, i.e. the sorption rate  
430 constant, the sorbing blood components-water partition coefficient and the biotransformation  
431 kinetics, it can be concluded from the modeling results that for most chemicals significant  
432 limitations due to slow binding kinetics appear unlikely.

433

### 434 **Conclusion**

435 The derived experimental dataset on binding kinetics in plasma shows that the sorption rate  
436 constants for the investigated test chemicals are fast enough to prevent any limitations. The  
437 generic modeling analysis further indicates that this result seems to be valid for most  
438 chemicals. Only for extreme parameter combinations in terms of chemical hydrophobicity and  
439 assumed rate constants for plasma binding, respiratory uptake of chemicals is limited due to  
440 slow binding kinetics. In these cases, the chemical then accumulates in the gills leading to  
441 increasing BCF values.

442 In general, however, limitation of uptake or other modeling related aspects (e.g. consideration  
443 of the potential first-pass effects in fish gills<sup>1</sup>) seem to be unlikely explanations for potential  
444 discrepancies between experimental and predicted BCF. In our opinion, it is more likely that  
445 explanations for such discrepancies could lie on the part of the *in vitro* methods used to  
446 determine biotransformation kinetics. For example, one particularly relevant aspect could be  
447 enzyme induction: Induction of biotransformation enzymes in the living animal over the  
448 duration of a BCF study is a factor that cannot be represented in *in vitro* assays lasting only a  
449 few hours. If significant enzyme induction occurs *in vivo*, the *in vitro* assays would  
450 underestimate the actual biotransformation and predictions using this biotransformation  
451 information would thus overestimate bioaccumulation.

452

### 453 **Acknowledgements**

454 We thank Markus Brinkmann for provision of rainbow trout plasma and Nina Klötzer for helpful  
455 lab assistance.

456 This research was financially supported by the German Environment Agency under FKZ  
457 3718 65 406 0 and by CEFIC LRI (ECO 47 project).

458

459

460

461 References

462

- 463 1. S. Krause and K.-U. Goss, Comparison of a simple and a complex model for BCF prediction  
 464 using *in vitro* biotransformation data, *Chemosphere*, 2020, **256**, 127048.
- 465 2. J. J. Trowell, F. A. P. C. Gobas, M. M. Moore and C. J. Kennedy, Estimating the  
 466 Bioconcentration Factors of Hydrophobic Organic Compounds from Biotransformation Rates  
 467 Using Rainbow Trout Hepatocytes, *Archives of Environmental Contamination and Toxicology*,  
 468 2018, **75**, 295-305.
- 469 3. J. W. Nichols, D. B. Huggett, J. A. Arnot, P. N. Fitzsimmons and C. E. Cowan-Ellsberry, Toward  
 470 improved models for predicting bioconcentration of well-metabolized compounds by  
 471 rainbow trout using measured rates of *in vitro* intrinsic clearance, *Environmental Toxicology  
 472 and Chemistry*, 2013, **32**, 1611-1622.
- 473 4. J. A. Arnot and F. A. P. C. Gobas, A Generic QSAR for Assessing the Bioaccumulation Potential  
 474 of Organic Chemicals in Aquatic Food Webs, *QSAR & Combinatorial Science*, 2003, **22**, 337-  
 475 345.
- 476 5. J. A. Arnot and F. A. P. C. Gobas, A food web bioaccumulation model for organic chemicals in  
 477 aquatic ecosystems, *Environmental Toxicology and Chemistry*, 2004, **23**, 2343-2355.
- 478 6. OECD, *Test No. 319A: Determination of in vitro intrinsic clearance using cryopreserved  
 479 rainbow trout hepatocytes (RT-HEP)*, 2018.
- 480 7. OECD, *Test No. 319B: Determination of in vitro intrinsic clearance using rainbow trout liver S9  
 481 sub-cellular fraction (RT-S9)*, 2018.
- 482 8. D. N. Brooke, M. J. Crookes and D. A. S. Merckel, Methods for predicting the rate constant for  
 483 uptake of organic chemicals from water by fish, *Environmental Toxicology and Chemistry*,  
 484 2012, **31**, 2465-2471.
- 485 9. J. Chen, J. E. Schiel and D. S. Hage, Noncompetitive peak decay analysis of drug–protein  
 486 dissociation by high-performance affinity chromatography, *Journal of Separation Science*,  
 487 2009, **32**, 1632-1641.
- 488 10. M. J. Yoo and D. S. Hage, Use of peak decay analysis and affinity microcolumns containing  
 489 silica monoliths for rapid determination of drug–protein dissociation rates, *Journal of  
 490 Chromatography A*, 2011, **1218**, 2072-2078.
- 491 11. X. Zheng, Z. Li, M. I. Podariu and D. S. Hage, Determination of rate constants and equilibrium  
 492 constants for solution-phase drug–protein interactions by ultrafast affinity extraction,  
 493 *Analytical Chemistry*, 2014, **86**, 6454-6460.
- 494 12. P. Li, Y. Fan, Y. Wang, Y. Lu and Z. Yin, Characterization of plasma protein binding dissociation  
 495 with online SPE-HPLC, *Scientific Reports*, 2015, **5**, 14866.
- 496 13. R. A. Weisiger, Dissociation from albumin: a potentially rate-limiting step in the clearance of  
 497 substances by the liver, *Proceedings of the National Academy of Sciences*, 1985, **82**, 1563-  
 498 1567.
- 499 14. L. M. Berezhkovskiy, Determination of hepatic clearance with the account of drug-protein  
 500 binding kinetics, *Journal of Pharmaceutical Sciences*, 2012, **101**, 3936-3945.
- 501 15. L. M. Berezhkovskiy, Some features of the kinetics and equilibrium of drug binding to plasma  
 502 proteins, *Expert Opinion on Drug Metabolism & Toxicology*, 2008, **4**, 1479-1498.
- 503 16. S. Krause and K.-U. Goss, The impact of desorption kinetics from albumin on hepatic  
 504 extraction efficiency and hepatic clearance: a model study, *Archives of Toxicology*, 2018, **92**,  
 505 2175-2182.
- 506 17. J. A. Jansen, Influence of plasma protein binding kinetics on hepatic clearance assessed from  
 507 a “tube” model and a “well-stirred” model, *Journal of Pharmacokinetics and  
 508 Biopharmaceutics*, 1981, **9**, 15-26.
- 509 18. M. Yoon, H. J. Clewell, 3rd and M. E. Andersen, Deriving an explicit hepatic clearance  
 510 equation accounting for plasma protein binding and hepatocellular uptake, *Toxicol In Vitro*,  
 511 2013, **27**, 11-15.

- 512 19. S. Krause, N. Ulrich and K.-U. Goss, Desorption kinetics of organic chemicals from albumin,  
513 *Archives of Toxicology*, 2018, **92**, 1065-1074.
- 514 20. B. I. Escher, C. E. Cowan-Ellsberry, S. Dyer, M. R. Embry, S. Erhardt, M. Halder, J. H. Kwon, K.  
515 Johanning, M. T. Oosterwijk, S. Rutishauser, H. Segner and J. Nichols, Protein and lipid  
516 binding parameters in rainbow trout (*Oncorhynchus mykiss*) blood and liver fractions to  
517 extrapolate from an *in vitro* metabolic degradation assay to *in vivo* bioaccumulation potential  
518 of hydrophobic organic chemicals, *Chemical Research in Toxicology*, 2011, **24**, 1134-1143.
- 519 21. P. Poulin, F. J. Burczynski and S. Haddad, The Role of Extracellular Binding Proteins in the  
520 Cellular Uptake of Drugs: Impact on Quantitative In Vitro-to-In Vivo Extrapolations of Toxicity  
521 and Efficacy in Physiologically Based Pharmacokinetic-Pharmacodynamic Research, *Journal of*  
522 *Pharmaceutical Sciences*, 2016, **105**, 497-508.
- 523 22. J.-H. Kwon, H.-J. Lee and B. I. Escher, Bioavailability of hydrophobic organic chemicals on an  
524 *in vitro* metabolic transformation using rat liver S9 fraction, *Toxicology in Vitro*, 2020, **66**,  
525 104835.
- 526 23. H. Laue, L. Hostettler, R. Badertscher, K. Jenner, G. Sanders, J. Arnot and A. Natsch,  
527 Examining Uncertainty in *in Vitro-in Vivo* Extrapolation Applied in Fish Bioconcentration  
528 Models, *Environmental Science & Technology*, 2020, **54**, 9483-9494.
- 529 24. M. Bteich, P. Poulin and S. Haddad, The potential protein-mediated hepatic uptake:  
530 discussion on the molecular interactions between albumin and the hepatocyte cell surface  
531 and their implications for the *in vitro*-to-*in vivo* extrapolations of hepatic clearance of drugs,  
532 *Expert Opinion on Drug Metabolism & Toxicology*, 2019, **15**, 633-658.
- 533 25. N. I. Kramer, J. C. H. van Eijkeren and J. L. M. Hermens, Influence of albumin on sorption  
534 kinetics in solid-phase microextraction: consequences for chemical analyses and uptake  
535 processes, *Analytical Chemistry*, 2007, **79**, 6941-6948.
- 536 26. P. Mayer, M. M. Fernqvist, P. S. Christensen, U. Karlson and S. Trapp, Enhanced Diffusion of  
537 Polycyclic Aromatic Hydrocarbons in Artificial and Natural Aqueous Solutions, *Environmental*  
538 *Science & Technology*, 2007, **41**, 6148-6155.
- 539 27. T. L. ter Laak, J. C. H. van Eijkeren, F. J. M. Busser, H. P. van Leeuwen and J. L. M. Hermens,  
540 Facilitated Transport of Polychlorinated Biphenyls and Polybrominated Diphenyl Ethers by  
541 Dissolved Organic Matter, *Environmental Science & Technology*, 2009, **43**, 1379-1385.
- 542 28. P. Mayer, U. Karlson, P. S. Christensen, A. R. Johnsen and S. Trapp, Quantifying the Effect of  
543 Medium Composition on the Diffusive Mass Transfer of Hydrophobic Organic Chemicals  
544 through Unstirred Boundary Layers, *Environmental Science & Technology*, 2005, **39**, 6123-  
545 6129.
- 546 29. S. Krause and K.-U. Goss, *In Vitro-in Vivo* Extrapolation of Hepatic Metabolism for Different  
547 Scenarios-a Toolbox, *Chemical Research in Toxicology*, 2018, **31**, 1195-1202.
- 548 30. H. Laue, H. Gfeller, K. J. Jenner, J. W. Nichols, S. Kern and A. Natsch, Predicting the  
549 bioconcentration of fragrance ingredients by rainbow trout using measured rates of *in vitro*  
550 intrinsic clearance, *Environmental science & technology*, 2014, **48**, 9486-9495.
- 551 31. S. Endo, T. N. Brown and K.-U. Goss, General model for estimating partition coefficients to  
552 organisms and their tissues using the biological compositions and polyparameter linear free  
553 energy relationships, *Environmental Science & Technology*, 2013, **47**, 6630-6639.
- 554 32. L. J. Saunders, G. Diaz-Blanco, Y.-S. Lee, S. V. Otton and F. A. P. C. Gobas, Hepatic Clearance  
555 Binding Terms of Hydrophobic Organic Chemicals in Rainbow Trout: Application of a  
556 Streamlined Sorbent-Phase Dosing Method, *Environmental Science & Technology Letters*,  
557 2020, **7**, 672-676.
- 558 33. M. Halder, A. Lostia and A. Kienzler, EURL ECVAM Fish *In Vitro* Intrinsic Clearance  
559 Database. *Journal*, 2018.

560 -